JCTC Journal of Chemical Theory and Computation

Rotational *g* Tensors Calculated Using Hybrid Exchange-Correlation Functionals with the Optimized Effective Potential Approach

Ola B. Lutnæs,[†] Andrew M. Teale,[‡] Trygve Helgaker,[†] and David J. Tozer*[,‡]

Department of Chemistry, University of Oslo, P.O. Box 1033, Blindern, N-0315 Oslo, Norway, and Department of Chemistry, University of Durham, South Road, Durham, DH1 3LE United Kingdom

Received February 2, 2006

Abstract: The calculation of rotational *g* tensors using density functional theory (DFT) with hybrid exchange-correlation functionals is considered. A total of 143 rotational *g* tensor elements in 58 molecules (67 isotopic combinations) are calculated using three standard hybrid functionals. Tensor elements determined using an uncoupled approach with orbitals and eigenvalues calculated from the multiplicative optimized effective potential (OEP) constitute a significant improvement over those determined in the conventional coupled manner with a nonmultiplicative exchange-correlation operator. Relative to experimental results, mean absolute errors are reduced by a factor of 2; mean errors and standard deviations are reduced by more than a factor of 3. The results are also an improvement over those determined using a generalized gradient-approximation functional optimized for magnetic response properties. The influence of orbital exchange is investigated for a representative subset of molecules, yielding an optimal amount near 0.3. Rotational *g* tensors are also determined from coupled-cluster electron densities using a combined DFT/wave-function approach. Being substantially more expensive, they do not offer a notable improvement on the pure DFT values from OEP-based hybrid calculations.

1. Introduction and Background

A rotating molecule acquires a magnetic moment proportional to its angular momentum. In an external magnetic field, the Zeeman interaction between this magnetic moment and the external magnetic induction causes a shift in the rotational energy levels, as observed by molecular beam[1] and microwave Zeeman experiments.[2,3] In atomic units (as used throughout this paper), the energy shift is conventionally expressed as

$$\Delta E = -\mu_N \mathbf{B}^T \mathbf{g} \mathbf{J} \tag{1}$$

where μ_N is the nuclear magneton, **B** is the external magnetic induction, **J** is the angular momentum of the molecule with respect to its center of mass, and **g** is the dimensionless 3×3 rotational *g* tensor. The *g* tensor can be evaluated as the second derivative of the electronic energy *E* with respect to **B** and **J**:

$$\mathbf{g} = -\frac{1}{\mu_N} \frac{\partial^2 E(\mathbf{B},\mathbf{J})}{\partial \mathbf{B} \partial \mathbf{J}}\bigg|_{\mathbf{B},\mathbf{J}=0} \tag{2}$$

The calculation of *g* tensors is thus similar to that of other singlet second-order magnetic response properties such as nuclear magnetic resonance (NMR) shielding constants, spin-rotation constants, and magnetizabilities. Indeed, in the center-of-mass coordinate system,[4] the *g* tensor can be determined directly from the magnetizability

$$\boldsymbol{\xi} = -\frac{\partial^2 E(\mathbf{B})}{\partial \mathbf{B}^2}\bigg|_{\mathbf{B}=0} \tag{3}$$

* Corresponding author fax: 0191 384 4737; e-mail: D.J.Tozer@Durham.ac.uk.
[†] University of Oslo.
[‡] University of Durham.

10.1021/ct060038n CCC: $33.50
Published on Web 04/15/2006

using the relation

$$\mathbf{g} = -\frac{2}{\mu_N}\xi_{CM}^{para}\,\mathbf{I}_{nuc}^{-1} + \frac{1}{2\mu_N}\sum_K Z_K\,(\mathbf{R}_K^T\mathbf{R}_K\mathbf{I}_3 - \mathbf{R}_K\mathbf{R}_K^T)\mathbf{I}_{nuc}^{-1} \quad (4)$$

where ξ_{CM}^{para} is the paramagnetic contribution to the magnetizability calculated with the gauge origin at the center of mass, $\mathbf{I}_{nuc}$ is the moment-of-inertia tensor, and Z_K is the charge of nucleus K at position $\mathbf{R}_K$ relative to the center of mass. This relation arises because the paramagnetic contributions to the g tensor and to the magnetizability (with the gauge origin at the center of mass) are proportional to each other, $\mathbf{g}^{para} = -2\xi_{CM}^{para}\mathbf{I}_{nuc}^{-1}/\mu_N$, as follows by comparing the first-order electronic perturbations generated by the external magnetic field $\mathbf{B}$ and by the rotationally induced magnetic field $-2\mathbf{I}_{nuc}^{-1}\mathbf{J}$. The paramagnetic contribution ξ_{CM}^{para} is straightforwardly obtained from the total magnetizability (calculated with London orbitals) ξ^{LAO}, by subtracting the diamagnetic (expectation value) contribution ξ_{CM}^{dia}. For further details regarding the theory and computation of rotational g tensors, see ref 4.

The high accuracy obtained in the experimental determination of rotational g tensors makes them an excellent test case for quantum-chemical theories. Indeed, a wide range of electronic-structure methods have been used to calculate g tensors, including Hartree−Fock (HF) theory;[4−7] multiconfigurational self-consistent field (MCSCF) theory;[8−15] Møller−Plesset theory to second,[14,16,17] third,[14,16] and fourth orders[14] (MP2, MP3, and MP4); linearized coupled-cluster doubles (L-CCD) theory;[16] coupled-cluster singles-and-doubles (CCSD) theory;[14] the second-order polarization propagator approximation (SOPPA);[14,18−20] the coupled-cluster polarization propagator approximation (CCSDPPA);[21−24] the SOPPA using CCSD amplitudes [SOPPA(CCSD)];[14,25] full configuration-interaction (FCI) theory;[26−28] and density functional theory (DFT).[13,29,30] DFT is particularly attractive because of its low computational cost. Recently, Wilson et al.[30] presented an extensive assessment of DFT rotational g tensors, using a range of exchange-correlation functionals. They considered the local density approximation (LDA), the Becke−Lee−Yang−Parr (BLYP)[31] generalized gradient approximation (GGA), and the Becke−3-parameter−Lee−Yang−Parr (B3LYP)[32] hybrid functional. They also considered the Keal−Tozer (KT2) GGA functional,[33] which was specifically designed to yield good quality magnetic response parameters. In particular, this functional has been shown to provide improved magnetizabilities compared to conventional approximations.[33] For rotational g tensors, Wilson et al.[30] observed that the quality improved in the order LDA < BLYP < B3LYP < KT2, reflecting the close relationship between the rotational g tensor and the magnetizability (see eq 4).

For the LDA and GGA functionals, the Kohn−Sham orbitals $\{\varphi_p(\mathbf{r})\}$ and eigenvalues $\{\epsilon_p\}$—the key quantities in the calculation of DFT response properties—are determined from the Kohn−Sham equations

$$\left[-\frac{1}{2}\nabla^2 + v_s(\mathbf{r})\right]\varphi_p(\mathbf{r}) = \epsilon_p\,\varphi_p(\mathbf{r}) \quad (5)$$

where $v_s(\mathbf{r})$ is a multiplicative one-electron potential

$$v_s(\mathbf{r}) = v_{ext}(\mathbf{r}) + v_J(\mathbf{r}) + v_{xc}(\mathbf{r}) \quad (6)$$

comprising external, Coulomb, and exchange-correlation components, respectively. The LDA and GGA magnetic Hessian, which determines the imaginary component of the orbital response, is diagonal, and so NMR shielding and spin-rotation constants as well as magnetizabilities and rotational g tensors are determined in an uncoupled manner. The whole approach is rigorously Kohn−Sham theory.

By contrast, for hybrid functionals such as B3LYP, which combines a GGA functional with an amount ξ of exact orbital exchange, the standard implementation in all widely used programs is not strictly Kohn−Sham theory. Specifically, rather than containing a multiplicative exchange-correlation potential as in eq 5, the orbital equations involve the scaled nonmultiplicative Hartree−Fock exchange operator

$$\left[-\frac{1}{2}\nabla^2 + v_s(\mathbf{r})\right]\varphi_p(\mathbf{r}) - \xi\int\frac{\rho_1(\mathbf{r},\mathbf{r}')}{|\mathbf{r}-\mathbf{r}'|}\,\varphi_p(\mathbf{r}')\,d\mathbf{r}' = \epsilon_p\,\varphi_p(\mathbf{r}) \quad (7)$$

where $\rho_1(\mathbf{r},\mathbf{r}')$ is the one-particle density matrix and the $v_{xc}(\mathbf{r})$ part of $v_s(\mathbf{r})$ (see eq 6) is the multiplicative potential associated with the GGA component of the functional. The resulting magnetic Hessian is nondiagonal, and so magnetic properties are determined in a coupled manner. This was the approach used for the B3LYP rotational g tensor calculations of Wilson et al.[30]

There has recently been much interest[34−42] in determining uncoupled second-order magnetic properties from hybrid functionals using a rigorous Kohn−Sham equation of the form of eq 5. The high-quality results obtainable from such an approach were first demonstrated for shielding constants—Wilson and Tozer[34] determined multiplicative potentials from electron densities with the Zhao−Morrison−Parr (ZMP) approach[43] and used the resulting orbitals and eigenvalues to determine uncoupled shieldings. When hybrid functional DFT densities were used, the ZMP results for a series of small, highly correlated molecules were two to three times more accurate than those of conventional hybrid theory; the results were also a significant improvement on the uncoupled values of conventional GGA theory. Cohen et al.[37] subsequently demonstrated that essentially identical shieldings are obtained when the potentials are determined using the rigorous optimized effective potential (OEP) approach.[44] Similar improvements have been observed for chemical shifts[35] and magnetizabilities,[36] and so analogous improvements are also anticipated for rotational g tensors. See refs 38−42 for more recent studies using alternative potential constructions.

The aim of the present study is to quantify the improvement in rotational g tensors. Specifically, we shall use the OEP method to determine multiplicative potentials associated with the B3LYP, B97-2,[45] and B97-3[46] hybrid functionals and then use the orbitals and eigenvalues from a rigorous Kohn−Sham equation of the form of eq 5 to determine uncoupled rotational g tensors. The results will be compared

with the conventional g tensors, determined in a coupled manner with a nonmultiplicative exchange-correlation operator as in eq 7, as well as with the uncoupled results from the KT2 GGA functional.[33] All results will be compared with experimental values, mentioning, where possible, the effect of zero-point vibrational corrections. We shall also investigate the influence of orbital exchange and determine rotational g tensors directly from ab initio coupled-cluster electron densities using the Wu−Yang (WY) approach.[47] We commence by summarizing the OEP and WY approaches and providing some computational details in section 2. The results of our calculations are presented in section 3. Conclusions are presented in section 4.

2. Theory and Computational Details

The OEP method[44] is the rigorous approach for handling orbital-dependent (e.g., hybrid) functionals in Kohn−Sham theory. The aim of the OEP method is to find the multiplicative potential, $v_s(\mathbf{r})$, in a rigorous Kohn−Sham equation of the form of eq 5, that minimizes the total electronic energy for the chosen exchange-correlation functional. We have implemented the OEP method, using the approach of Yang and Wu,[48,49] in the CADPAC quantum-chemistry code.[50] Specifically, the potential is written

$$v_s(\mathbf{r}) = v_{ext}(\mathbf{r}) + v_0(\mathbf{r}) + \sum_t b_t\, g_t(\mathbf{r}) \tag{8}$$

where $v_{ext}(\mathbf{r})$ is the external potential, $v_0(\mathbf{r})$ is a fixed reference potential, and the final term is an expansion in an auxiliary basis of Gaussian functions $g_t(\mathbf{r})$. The only unknown parameters are the coefficients $\{b_t\}$, which are determined by a direct minimization of the total electronic energy with respect to these parameters, using an approximate Newton scheme.[49] For the reference potential, we use the Fermi−Amaldi potential constructed using the Hartree−Fock density of the system,

$$v_0(\mathbf{r}) = \left(1 - \frac{1}{N}\right) v_J^{HF}(\mathbf{r}) \tag{9}$$

where N is the number of electrons and $v_J^{HF}(\mathbf{r})$ is the Coulomb potential of the Hartree−Fock density.

While the OEP method provides the rigorous scheme for orbital-dependent functionals in DFT, the constrained-search formulation[51] provides an alternative method for determining multiplicative exchange-correlation potentials. In this method, the noninteracting kinetic energy is minimized subject to the constraint that the orbitals yield a supplied electron density. Wu and Yang have proposed a particular method[47] for such calculations, denoted WY, which is computationally similar to the OEP method and formally equivalent to the ZMP method. We have also implemented this approach in CADPAC. For a given input density $\rho_{in}(\mathbf{r})$, the solution to the problem can be recast as the unconstrained maximization of the functional

$$W_s[\Phi_{det}, v(\mathbf{r})] = 2\sum_i^{N/2}\left\langle \varphi_i \middle| -\frac{1}{2}\nabla^2 \middle| \varphi_i \right\rangle + \int d\mathbf{r}\, \{v_{ext}(\mathbf{r}) + v_0(\mathbf{r})\}\{\rho(\mathbf{r}) - \rho_{in}(\mathbf{r})\} + \int d\mathbf{r} \sum_t b_t\, g_t(\mathbf{r})\, \{\rho(\mathbf{r}) - \rho_{in}(\mathbf{r})\} \tag{10}$$

with respect to $\{b_t\}$, where the orbitals are obtained from a Kohn−Sham equation of the form of eq 5 with the potential defined as in eq 8 and $\rho(\mathbf{r})$ is the density constructed from these orbitals. The maximization is carried out using a quasi-Newton algorithm similar to the one used for the OEP approach. For further details, see ref 47.

The WY method can be applied to a DFT density associated with a hybrid exchange-correlation functional. As demonstrated by Cohen et al.,[37] the resulting WY shielding constants are very close to those obtained by applying the OEP method to the same functional. However, the WY method has the important advantage that it does not require explicit knowledge of the exchange-correlation functional associated with the input density. In the present work, we shall therefore also calculate g tensors using potentials determined from high-quality Brueckner-doubles (BD) coupled-cluster densities.

A key feature of the OEP and WY schemes is that $v_s(\mathbf{r})$ is expressed analytically through eq 8. Once optimal $\{b_t\}$ coefficients have been determined, it is therefore straightforward to reconstruct this potential in any electronic-structure program. Specifically, we here determine these coefficients using CADPAC and then read the values into a modified version of the DALTON program,[52] which assembles the potential using the same geometry, reference potential, and orbital and auxiliary basis sets. The resulting Kohn−Sham equations are then solved [by a single diagonalization because $v_s(\mathbf{r})$ does not depend on the orbitals], and the orbitals and eigenvalues are used to compute the uncoupled rotational g tensors.

The main advantage of this two-code approach is that it allows us to use rotational London atomic orbitals in the g-tensor evaluation to ensure fast basis-set convergence and gauge-independent results,[4] noting that such orbitals are essential for molecules of the size considered in this work and that they are not available in the CADPAC program. The approach also allows the enhanced property calculations of DALTON to be exploited in future investigations. Our implementation was checked by confirming that the converged one-electron eigenvalues in DALTON agreed with those of the CADPAC OEP/WY calculation, to within numerical integration error. Property calculations were checked by comparing single-origin magnetizability calculations in DALTON and CADPAC. The London-orbital calculations were checked by confirming gauge-origin invariance and by comparing large-basis single-origin magnetizabilities with London-orbital magnetizabilities for small molecules.

We closely follow the study of Wilson et al.,[30] using the same aug-cc-pVTZ basis[53−55] (but with Cartesian rather than spherical functions) and the same molecules, omitting the largest four because of computational limitations. The 58

Table 1. Molecules Considered in This Study

carbon monoxide [CO], carbon sulfide [CS], carbon selenide [CSe], hydrogen cyanide [$HC^{15}N$], fluoro cyanide [$FC^{15}N$], chloro cyanide [$ClC^{15}N$], bromo cyanide [$BrC^{15}N$], carbonyl sulfide [OCS, $OC^{34}S$, $O^{13}CS$], nitrous oxide [$^{15}N^{15}NO$, $^{14}N^{14}NO$], carbonyl selenide [$OC^{80}Se$, $OC^{76}Se$], methylidene phosphine [HCP, DCP], hydrogen boron sulfide [HBS], fluoro acetylene [FCCH], chloro acetylene [$^{35}ClCCH$, $^{37}ClCCH$], bromo acetylene [$^{79}BrCCH$, $^{81}BrCCH$], ammonia [$^{15}NH_3$], trifluoromethane [CHF_3], methylisocyanide [$CH_3{}^{14}NC$], acetonitrile [$CH_3C^{15}N$, $CH_3C^{14}N$, $CD_3C^{14}N$], fluoromethane [CH_3F], chloromethane [CH_3Cl], acrolein [CH_2CHCHO], propene [CH_2CHCH_3], propynal [HCCCHO], dimethyl ether [CH_3OCH_3], dimethylsulfane [CH_3SCH_3], acetaldehyde [CH_3CHO], formaldehyde [H_2CO], thioformaldehyde [H_2CS], formic acid [HCOOH], formamide [$HCONH_2$], glycoaldehyde [CH_2OHCHO], methyl formate [$HCOOCH_3$], ketene [H_2CCO], difluoromethane [CH_2F_2], carbonic difluoride [F_2CO], formyl fluoride [HFCO], fluoroethene [$CFHCH_2$], 1,1-difluoroethene [CF_2CH_2], *cis*-difluoroethene [CFHCFH], fluoroethane [CFH_2CH_3], trifluoroethene [CF_2CFH], ozone [O_3], sulfur dioxide [SO_2], difluorooxide [F_2O], hypofluoros acid [HOF], water [H_2O], hydrogendisulfide [H_2S], methylenecyclopropane [C_4H_6], cyclopropene [C_3H_4], aziridine [C_2H_5N], oxirane [C_2H_4O], thiirane [C_2H_4S], cyclopropenone [C_3H_2O], methylcyclopropene [C_4H_6], cyclobutene [C_4H_6], oxetane [C_3H_6O], β-propiolactone [$C_3H_4O_2$]

molecules considered (67 isotopic combinations, 143 tensor elements) are listed in Table 1. Rotational g tensors are known to be sensitive to geometry,[13] although Wilson et al. observed that the relative performance of different DFT functionals was the same whether optimized or experimental geometries were used. We only consider experimental geometries here, taken from ref 30 apart from ozone, for which we use $r = 1.2717$ Å and $\theta = 116.78°$.[56] With the exception of ammonia and thioformaldehyde, we compare results with the experimental g tensors compiled by Wilson et al.[30] For ammonia, we found experimental results with smaller error bars;[57] for thioformaldehyde, we used -5.2602 for the dominant diagonal element of the g tensor, noting that Wilson et al. used an incorrect value of -5.6202 because of a typographical error in the original experimental paper.[58]

We commenced by performing extensive investigations into the choice of the auxiliary Gaussian basis functions $g_t(\mathbf{r})$ for the expansion of the potential in eq 8 and the value of the filter in the singular-value decomposition (SVD) procedure used to construct the inverse Hessian in the optimization schemes. For the auxiliary basis, we considered both even-tempered basis sets and the use of the primary orbital basis. We found that the primary orbital basis was not sufficiently large, with deviations of more than 2% from converged results for simple molecules. For the even-tempered auxiliary basis sets, s, p, d, and f functions were placed on all atom centers, with exponents λ^{n_s}, λ^{n_p}, and so forth, where λ is a universal base and n_s, n_p, and so forth are (negative and positive) integers that define the range of the functions. After some investigations, a base of $\lambda = 2$ was used for all functions with the range chosen such that the exponents span those of the orbital basis, with the lowest exponent multiplied by 0.1. Because very large exponents led to a spurious structure in the OEP potential, functions with exponents larger than 2^6 were discarded, noting that the removal of the high exponents affected the g tensors less than a change in the orbital basis from triple- to quadruple-ζ. For the SVD filter, an analysis of the shape of the potentials and the dependence of the highest occupied molecular orbital eigenvalue led us to conclude that a value of 10^{-4} was appropriate. Once again, the effect of changing the filter was smaller than the orbital-basis incompleteness error.

To test our auxiliary basis set, we used the OEP procedure to calculate rotational g tensors for the KT2 GGA functional. Because the KT2 Kohn−Sham equation already takes the form of eq 5, the OEP procedure should, in the limit of a complete auxiliary basis, yield the same solution. A comparison of conventional uncoupled KT2 g tensors with those determined using the OEP orbitals and eigenvalues therefore provides a measure of the quality of the auxiliary basis set. Calculations were performed on a representative subset (specifically, the molecules considered in section 3.1). For the 15 tensor components, the average deviation from conventional KT2 values was 0.1%, with a maximum deviation of 0.3%.

3. Results and Discussion

Table 2 lists the mean absolute error (MAE), mean error (ME), percentage mean absolute error (PMAE), and standard deviation (SD) for the calculated rotational g tensors of the molecules in Table 1, compared with experimental values. Following Wilson et al.,[30] we present the error analysis both including and omitting the ozone molecule, because of its significant multireference character. Whereas the values denoted B3LYP, B97-2, and B97-3 refer to g tensors determined in a conventional, coupled manner using orbitals and eigenvalues from eq 7, those denoted O-B3LYP, O-B97-2, and O-B97-3 are the new values, determined in an uncoupled manner, using orbitals and eigenvalues from eq

Table 2. Mean Absolute Error (MAE), Mean Error (ME), Percentage Mean Absolute Error (PMAE), and Standard Deviation (SD) for Rotational g Tensor Elements, Relative to Experimental Values

	including ozone				excluding ozone			
	MAE	ME	PMAE	SD	MAE	ME	PMAE	SD
KT2	0.0082	−0.0043	10.9	0.0203	0.0078	−0.0048	11.1	0.0197
B3LYP	0.0153	−0.0133	11.3	0.0636	0.0107	−0.0087	11.2	0.0347
B97-2	0.0125	−0.0084	8.8	0.0583	0.0079	−0.0037	8.7	0.0224
B97-3	0.0149	−0.0107	9.2	0.0735	0.0091	−0.0049	9.1	0.0297
O-B3LYP	0.0077	−0.0037	12.0	0.0189	0.0070	−0.0046	12.2	0.0162
O-B97-2	0.0057	0.0013	7.1	0.0165	0.0048	0.0003	7.2	0.0120
O-B97-3	0.0064	0.0018	6.8	0.0214	0.0049	0.0003	6.9	0.0120

Table 3. Rotational g Tensor Components for the Ozone Molecule

	g_{xx}	g_{yy}	g_{zz}
KT2	−2.9230	−0.2313	−0.0792
B3LYP	−3.6369	−0.2657	−0.0783
B97-2	−3.6351	−0.2635	−0.0751
B97-3	−3.7980	−0.2729	−0.0754
O-B3LYP	−2.8729	−0.2259	−0.0782
O-B97-2	−2.8508	−0.2226	−0.0752
O-B97-3	−2.7752	−0.2195	−0.0754
exptl.	−2.9877	−0.2295	−0.0760
exptl.[a]	−2.9169	−0.2277	−0.0746

[a] Experimental results with calculated zero-point vibrational contributions (from ref 13) removed.

5 with the multiplicative OEP exchange-correlation potential. The results of all individual calculations, together with experimental data, are available in the Supporting Information.

For hybrid functionals, the uncoupled OEP approach gives significantly improved g tensors compared with those of the conventional approach. When all of the molecules are included, mean absolute errors reduce by at least a factor of 2 in moving from B3LYP, B97-2, and B97-3 to O-B3LYP, O-B97-2, and O-B97-3, respectively, while mean errors and standard deviations reduce by more than a factor of 3. The percentage mean absolute error reduces for the latter two functionals. The percentage errors are particularly large for tensor elements in molecules such as dimethyl ether and fluorethane. When ozone is excluded from the analysis, the improvement is more modest, reflecting the fact that ozone is particularly poorly described by conventional calculations. This is to be expected because the method has a close relationship (because of the fraction of orbital exchange) to coupled Hartree−Fock theory, which is very poor because of the multireference nature of this molecule. By contrast, ozone is not an especially challenging case for the OEP-based calculations. To quantify this, Table 3 presents rotational g tensors for ozone, compared with experimental values, both including and excluding zero-point vibrational contributions. For the g_{zz} component, which is described well by the conventional hybrid calculations, the OEP calculations yield essentially the same results. For the g_{xx} and g_{yy} components, which are in error with the conventional approach, the OEP calculations are a notable improvement. The improvement in g_{xx} is particularly pronounced.

With all molecules included, the quality as measured by the MAE can be summarized as

$$\text{B3LYP} < \text{B97-3} < \text{B97-2} < \text{KT2} < \text{O-B3LYP} < \text{O-B97-3} < \text{O-B97-2} \quad (11)$$

with the top method, O-B97-2, exhibiting MAE, ME, PMAE, and SD values of 0.0057, 0.0013, 7.1%, and 0.0165, respectively. Figure 1 quantifies the correlation between the O-B97-2 and experimental g tensors; the slope and intercept of the linear trendline are 1.0102 and −0.0002, respectively, with $R^2 = 0.9993$. When O_3 is excluded, there is little to choose between O-B97-2 and O-B97-3 as the top method. Whether ozone is included or not, the KT2 functional, which

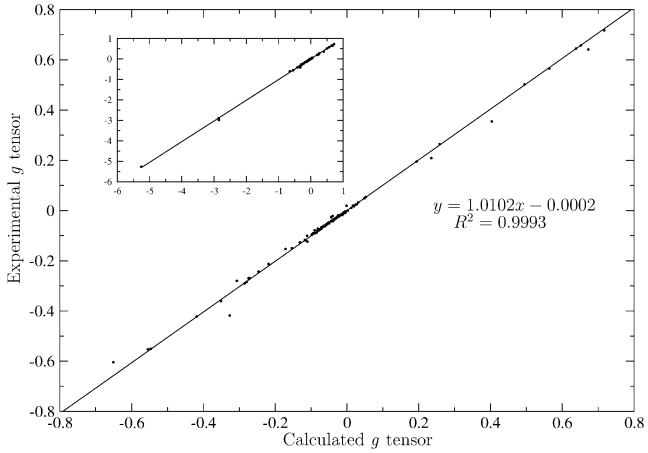

Figure 1. Correlation of O-B97-2 rotational g tensors with experimental values. The inset includes the entire range of g tensors.

was found to be the most accurate DFT method in the study of Wilson et al.,[30] is outperformed by the OEP-based hybrid functionals.

The errors are particularly small for the 22 linear molecules in the data set. For this subset, O-B97-3 gives the lowest MAE of just 0.0011, followed by O-B97-2 (0.0013), KT2 (0.0017), O-B3LYP (0.0018), B97-2 (0.0040), B97-3 (0.0049), and B3LYP (0.0050). The smallest errors are approaching the experimental error bars. Considering individual linear molecules, the OEP-based hybrid values are a particular improvement on the conventional hybrid results for CO, CS, CSe, and HCN. Other g-tensor elements for which the OEP results represent a sizable improvement are the large components in thioformaldehyde, formaldehyde, and sulfur dioxide. Indeed, it was the analysis of our OEP results that highlighted the error in the quoted thioformaldehyde experimental number of refs 3 and 30. After ozone, the most significant error with O-B97-2 occurs for the largest component of the ketene g tensor. The O-B97-2 value (−0.3267) is well-above the experimental value (−0.4182) and is even less accurate than the conventional B97-2 result (−0.3601). The discrepancy is evident in Figure 1. We have confirmed that this discrepancy does not arise from inadequacies in the orbital or auxiliary basis sets. It is interesting to note that the KT2 functional is also relatively poor for ketene (−0.3433).

It is pertinent to comment on the effect of zero-point vibrational corrections (ZPVCs) on rotational g tensors. The experimental data used in the above comparison with DFT do not include ZPVCs; they contain vibrational as well as electronic contributions. Vibrational corrections are scarce, although we are aware[13,15] of MCSCF values for NH_3, H_2O, HOF, and O_3 and a Hartree−Fock value for H_2S. To examine the importance of such corrections, we have computed errors for these molecules, comparing them with corrected as well as uncorrected experimental data. For O-B3LYP, O-B97-2, and O-B97-3, inclusion of the ZPVC reduces the MAE, by an average of 6%. For B3LYP, B97-2, and B97-3, by contrast, the correction increases the error, by an average of 14%. For all six methods, the PMAEs actually increase slightly because of the small g-tensor components, although

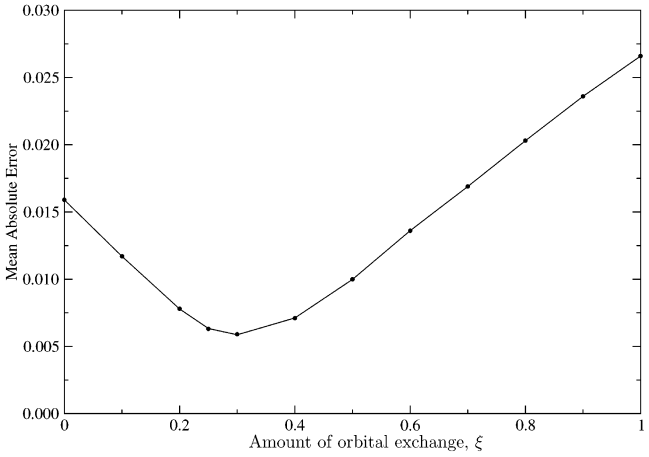

Figure 2. Mean absolute error for a subset of eight molecules (see text) as a function of the amount of orbital exchange, ξ.

the average increase is smaller for the OEP-based methods. Explicit values for ozone are presented in Table 3. This analysis, albeit based on limited data, supports our conclusions regarding the improved quality of predictions from OEP-based hybrid calculations.

3.1. Influence of Orbital Exchange. In ref 59, we investigated the influence of the amount of orbital exchange ξ (see eq 7) on uncoupled shielding constants determined using orbitals and eigenvalues associated with a multiplicative exchange-correlation potential. Using the ZMP exchange-correlation potential, we found that an amount $0.2 \leq \xi \leq 0.3$ was optimal, consistent with the amount used in common hybrid functionals such as B3LYP. By contrast, Arbuznikov and Kaupp[40] used the localized Hartree−Fock (LHF) approach[60] [equivalent to the common energy denominator approximation (CEDA)[61]] and instead found that an amount nearer 0.6 was optimal. These different optimal amounts of exact exchange reflect differences between the LHF and ZMP potentials. The reader is referred to refs 38 and 62 for further discussion on the differences between these and other potentials.

In the present investigation, we have used the OEP procedure to determine orbitals and eigenvalues for the series of functionals in ref 59, with different amounts of exchange $0 \leq \xi \leq 1$. From these potentials, we have determined uncoupled rotational g tensors for the representative subset of molecules CO, CSe, OCS, N_2O, NH_3, HOF, H_2O, and SO_2. Figure 2 presents the mean absolute error relative to experimental results as a function of ξ. In line with the NMR-shielding observations of ref 59, the best results are obtained with $\xi \approx 0.3$, which is consistent with previous observations highlighting the similarity of the ZMP and OEP potentials.[37,62]

3.2. *g* Tensors Calculated from Coupled-Cluster Densities. The results discussed so far have been pure DFT results. We complete this study by instead determining rotational g tensors directly from ab initio electron densities using the WY approach. Specifically, we calculate BD coupled-cluster relaxed densities and input them [$\rho_{in}(\mathbf{r})$ in eq 10] into our implementation of the WY procedure in CADPAC, which yields an optimal set of expansion parameters $\{b_t\}$. These are then transferred to DALTON as in the OEP calculations, and the uncoupled g tensor is evaluated. The results are denoted WY(BD).

We have considered the same subset of molecules as that in section 3.1; all results are presented in the Supporting Information. The conventional hybrids give mean absolute errors from 0.0127 (B97-2) to 0.0139 (B97-3), whereas the OEP errors are between 0.0068 (O-B97-3) and 0.0084 (O-B3LYP). The WY(BD) mean absolute error is slightly lower, at 0.0066. The WY(BD) results are of good quality but, of course, require the evaluation of the coupled-cluster relaxed density. The modest gain in accuracy is therefore associated with a significant increase in computational cost; the method is not practical for larger molecules. We also note that the WY(BD) results are poor for the ozone molecule. If this molecule is included in the subset, then the OEP methods are an improvement over WY(BD).

4. Conclusions

In line with previous studies of NMR shielding constants,[34,37] chemical shifts,[35] and magnetizabilities,[36] we have demonstrated that significantly improved rotational g tensors can be obtained with hybrid functionals by an uncoupled evaluation, using orbitals and eigenvalues from a rigorous Kohn−Sham equation, eq 5. Compared with the conventional approach, which uses a coupled formalism and nonmultiplicative exchange-correlation operator, eq 7, mean absolute errors are reduced by at least a factor of 2, whereas mean errors and standard deviations are reduced by more than a factor of 3. When ozone is omitted, the improvement is more modest, reflecting the fact that ozone is particularly poorly described by conventional calculations. Notably, the results are also an improvement over those from the KT2 GGA functional, which was developed with an emphasis on a high-quality magnetic response and which provided the highest quality in the study of Wilson et al.[30] The OEP calculations are more computationally demanding than those of the KT2 functional, requiring an implementation of the OEP methodology, although they do exhibit the favorable scaling of DFT. We have also demonstrated that, for a representative subset of molecules, optimal results are obtained with an amount of orbital exchange $\xi \approx 0.3$. When g tensors are determined from coupled-cluster electron densities, the improvement is only modest, at significant additional computational expense.

This study highlights the high-quality rotational g-tensor predictions possible within DFT; further investigations are under way. We are also using the ideas of this paper to investigate spin-rotation constants, which are related to shielding constants in the same way that g tensors are related to magnetizabilities. Results will be reported in a forthcoming publication.

Acknowledgment. We are grateful to D. J. D. Wilson for providing input geometry files for DALTON and to P. Salek for implementation of the B97-2 and B97-3 functionals in DALTON. This work has received support from the EPSRC (A.M.T. studentship) and the Norwegian National Research Council through a Strategic University Program in Quantum Chemistry grant (Grant No. 154011/420) and

through a grant of computer time from the program of Supercomputing. O.B.L. acknowledges the facilities provided by the University of Durham, during his six month visit.

Supporting Information Available: All calculated rotational *g* tensors and experimental data. This material is available free of charge via the Internet at http://pubs.acs.org.

References

(1) Ramsey, N. F. *Molecular Beams*; Clarendon Press: Oxford, U. K. ,2000.

(2) Flygare, W. H.; Benson, C. H. *Mol. Phys.* **1971**, *20*, 225−250.

(3) Flygare, W. H. *Chem. Rev.* **1974**, *74*, 653−687.

(4) Gauss, J.; Ruud, K.; Helgaker, T. *J. Chem. Phys.* **1996**, *105*, 2804−2812.

(5) Stevens, R. M.; Pitzer, R. M.; Lipscomb, W. N. *J. Chem. Phys.* **1963**, *38*, 550−560.

(6) Kelly, H. M.; Fowler, P. W. *Chem. Phys. Lett.* **1993**, *206*, 568−573.

(7) Ruud, K.; Helgaker, T. *Chem. Phys. Lett.* **1997**, *264*, 17−23.

(8) Ogilvie, J. F.; Cheah, S.-L.; Lee, Y.-P.; Sauer, S. P. A. *Theor. Chem. Acc.* **2002**, *108*, 85−97.

(9) Åstrand, P.-O.; Ruud, K.; Mikkelsen, K. V.; Helgaker, T. *Mol. Phys.* **1997**, *92*, 89−96.

(10) Åstrand, P.-O.; Ruud, K.; Mikkelsen, K. V.; Helgaker, T. *J. Chem. Phys.* **1999**, *110*, 9463−9468.

(11) Ruud, K.; Helgaker, T.; Jørgensen, P. *J. Chem. Phys.* **1997**, *107*, 10559−10606.

(12) Ruud, K.; Vaara, J.; Lounila, J.; Helgaker, T. *Chem. Phys. Lett.* **1998**, *297*, 467−474.

(13) Mohn, C. E.; Wilson, D. J. D.; Lutnæs, O. B.; Helgaker, T.; Ruud, K. *Adv. Quantum Chem.* **2005**, *50*, 77−90.

(14) Sauer, S. P. A. *Adv. Quantum Chem.* **2005**, *48*, 319−334.

(15) Ruud, K.; Åstrand P.-O.; Taylor, P. R. *J. Chem. Phys.* **2000** *112*, 2668−2683.

(16) Cybulski, S. M.; Bishop, D. M. *J. Chem. Phys.* **1997**, *106*, 4082−4090.

(17) Cybulski, S. M.; Bishop, D. M. *J. Chem. Phys.* **1993**, *100*, 2019−2026.

(18) Oddershede, J.; Sabin, J. R. *Chem. Phys.* **1988**, *122*, 291−296.

(19) Sauer, S. P. A.; Špirko, V.; Paidarová, I.; Oddershede, J. *Chem. Phys.* **1994**, *184*, 1−3.

(20) Sauer, S. P. A.; Špirko, V.; Oddershede, J. *Chem. Phys.* **1991**, *153*, 189−200.

(21) Sauer, S. P. A.; Ogilvie, J. F. *J. Phys. Chem.* **1994**, *98*, 8617−8621.

(22) Ogilvie, J. F.; Oddershede, J.; Sauer, S. P. A. *Chem. Phys. Lett.* **1994**, *228*, 183−190.

(23) Geertsen, J.; Scuseria, G. E. *J. Chem. Phys.* **1989**, *90*, 6486−6490.

(24) Sauer, S. P. A.; Oddershede, J.; Geertsen, J. *Mol. Phys.* **1992**, *76*, 445−465.

(25) Sauer, S. P. A. *Chem. Phys. Lett.* **1996**, *260*, 271−279.

(26) Ruud, K.; Åstrand, P.-O.; Helgaker, T.; Mikkelsen, K. V. *THEOCHEM* **1996**, *388*, 231−235.

(27) Åstrand, P.-O.; Ruud, K.; Mikkelsen, K. V.; Helgaker, T. *Chem. Phys. Lett.* **1997**, *271*, 163−166.

(28) Bak, K. L.; Sauer, S. P. A.; Oddershede, J.; Ogilvie, J. F. *Phys. Chem. Chem. Phys.* **2005**, *7*, 1747−1758.

(29) Wilson, P. J.; Amos, R. D.; Handy, N. C. *J. Mol. Struct.* **2000**, *506*, 335−342.

(30) Wilson, D. J. D.; Mohn, C. E.; Helgaker T. *J. Chem. Theory Comput.* **2005**, *1*, 877−888.

(31) Becke, A. D. *Phys. Rev. A* **1988**, *38*, 3098−3100. Lee, C.; Yang, W.; Parr, R. G. *Phys. Rev. B* **1988**, *37*, 785−789.

(32) Stephens, P. J.; Devlin, F. J.; Chabalowski, C. F.; Frisch, M. J. *J. Phys. Chem.* **1994**, *98*, 11623−11627. Becke, A. D. *J. Chem. Phys.* **1993**, *98*, 5648−5652.

(33) Keal, T. W.; Tozer, D. J. *J. Chem. Phys.* **2003**, *119*, 3015−3024.

(34) Wilson, P. J.; Tozer, D. J. *Chem. Phys. Lett.* **2001**, *337*, 341−348.

(35) Allen, M. J.; Keal, T. W.; Tozer, D. J. *Chem. Phys. Lett.* **2003**, *380*, 70−77.

(36) Wilson, P. J.; Tozer, D. J. *J. Mol. Struct.* **2002**, *602*−*603*, 191−197.

(37) Cohen, A. J.; Wu, Q.; Yang, W. *Chem. Phys. Lett.* **2004**, *399*, 84−88.

(38) Teale, A. M.; Tozer, D. J. *Chem. Phys. Lett.* **2004**, *383*, 109−114.

(39) Hieringer, W.; Della Sala, F.; Gorling, A. *Chem. Phys. Lett.* **2004**, *383*, 115−121.

(40) Arbuznikov, A. V.; Kaupp, M. *Chem. Phys. Lett.* **2004**, *386*, 8−16.

(41) Arbuznikov, A. V.; Kaupp, M. *Chem. Phys. Lett.* **2004**, *391*, 16−21.

(42) Arbuznikov, A. V.; Kaupp, M. *Int. J. Quantum Chem.* **2005**, *104*, 261−271.

(43) Zhao, Q.; Morrison, R. C.; Parr, R. G. *Phys. Rev. A* **1994**, *50*, 2138−2142.

(44) Sharp, R. T.; Horton, G. K. *Phys. Rev.* **1953**, *90*, 317. Talman, J. D.; Shadwick, W. F. *Phys. Rev. A* **1976**, *14*, 36−40.

(45) Wilson, P. J.; Bradley, T. J.; Tozer, D. J. *J. Chem. Phys.* **2001**, *115*, 9233−9242.

(46) Keal, T. W.; Tozer, D. J. *J. Chem. Phys.* **2005**, *123*, 121103.

(47) Wu, Q.; Yang, W. *J. Chem. Phys.* **2003**, *118*, 2498−2509.

(48) Yang, W.; Wu, Q. *Phys. Rev. Lett.* **2002**, *89*, 143002.

(49) Wu, Q.; Yang, W. *J. Theor. Comput. Chem.* **2003**, *2*, 627−638.

(50) Amos, R. D. *CADPAC 6.5, The Cambridge Analytic Derivatives Package*; Cambridge University: Cambridge, England, 1998.

(51) Levy, M. *Proc. Natl. Acad. Sci. U.S.A.* **1979**, *76*, 6062−6065.

(52) *DALTON*, release 2.0; 2005. See http://www.kjemi.uio.no/software/dalton/dalton.html (accessed June 2005).

(53) Kendall, R. A.; Dunning, T. H., Jr. *J. Chem. Phys.* **1992**, *96*, 6796−6806.

(54) Woon, D. E.; Dunning, T. H., Jr. *J. Chem. Phys.* **1993**, *98*, 1358−1371.

(55) Wilson, A. K.; Woon, D. E.; Peterson, K. A.; Dunning, T. H. *J. Chem. Phys.* **1999**, *110*, 7667−7676.

(56) Tanaka, T.; Morino, Y. *J. Mol. Spectrosc.* **1970**, *33*, 538−551.

(57) Hüttner, W.; Frank, U. E.; Majer, W.; Mayer, K.; Špirko, V. *Mol. Phys.* **1988**, *64*, 1233−1249.

(58) Rock, S. L.; Flygare, W. H. *J. Chem. Phys.* **1972**, *56*, 4723−4728.

(59) Wilson, P. J.; Tozer, D. J. *J. Chem. Phys.* **2002**, *116*, 10139−10147.

(60) Della Sala, F.; Görling, A. *J. Chem. Phys.* **2001**, *115*, 5718−5732.

(61) Gritsenko, O. V.; Baerends, E. J. *Phys. Rev. A* **2001**, *64*, 042506.

(62) Teale, A. M.; Tozer, D. J. *Phys. Chem. Chem. Phys.* **2005**, *7*, 2991−2998.

CT060038N